

RECEIVED BY DTIC SEP 13 1968

MASTER

COO-1198-564

THE FREQUENCY DEPENDENCE OF DISLOCATION DAMPING
IN B.C.C. NIOBIUM

Bidyut Kumar Ganguly

Department of Mining, Metallurgy and Petroleum Engineering
and Materials Research Laboratory
University of Illinois, Urbana, Illinois

August 1968

This is a technical information document based on a thesis submitted by Bidyut Kumar Ganguly in partial fulfillment of the requirements for the degree of Master of Science in Metallurgical Engineering in the Graduate College of the University of Illinois 1968. This research was supported in part by the U. S. Atomic Energy Commission under Contract AT(11-1)-1198.

DISCLAIMER

This report was prepared as an account of work sponsored by an agency of the United States Government. Neither the United States Government nor any agency Thereof, nor any of their employees, makes any warranty, express or implied, or assumes any legal liability or responsibility for the accuracy, completeness, or usefulness of any information, apparatus, product, or process disclosed, or represents that its use would not infringe privately owned rights. Reference herein to any specific commercial product, process, or service by trade name, trademark, manufacturer, or otherwise does not necessarily constitute or imply its endorsement, recommendation, or favoring by the United States Government or any agency thereof. The views and opinions of authors expressed herein do not necessarily state or reflect those of the United States Government or any agency thereof.

DISCLAIMER

Portions of this document may be illegible in electronic image products. Images are produced from the best available original document.

THE FREQUENCY DEPENDENCE OF DISLOCATION DAMPING
IN B.C.C. NIOBIUM

Bidyut Kumar Ganguly

Department of Mining, Metallurgy and
Petroleum Engineering

University of Illinois, 1968

ABSTRACT

The frequency dependence of the amplitude independent dislocation damping in high purity Niobium single crystals was measured in the megacycle frequency range. Measurements of the dislocation contribution to the elastic modulus were also carried out in this frequency range. The results are discussed in terms of a theoretical calculation which treats the dislocation as a pinned vibrating string which experiences a viscous drag proportional to its velocity. The data are consistent with a curve of the form

$$= K \frac{\omega \tau}{1 + \omega^2 \tau^2}$$

as calculated from the vibrating string model. On the high frequency side of the maximum the dislocation damping exhibited a ω^{-1} dependence as expected from the theory.

229

The effect of various interstitial solute contents on the damping was shown to be consistent with the calculated dependence of the damping on pinning point concentrations. The viscous damping constant was calculated from the damping and from etch pit determinations of the dislocation density to be about 9×10^{-5} dyne-sec per cm^2 . Within the experimental precision the modulus defect was found to be independent of frequency and to increase with increasing interstitial concentrations.

LEGAL NOTICE

This report was prepared as an account of Government sponsored work. Neither the United States, nor the Commission, nor any person acting on behalf of the Commission:

A. Makes any warranty or representation, expressed or implied, with respect to the accuracy, completeness, or usefulness of the information contained in this report, or that the use of any information, apparatus, method, or process disclosed in this report may not infringe privately owned rights; or

B. Assumes any liabilities with respect to the use of, or for damages resulting from the use of any information, apparatus, method, or process disclosed in this report.

As used in the above, "person acting on behalf of the Commission" includes any employee or contractor of the Commission, or employee of such contractor, to the extent that such employee or contractor of the Commission, or employee of such contractor prepares, disseminates, or provides access to, any information pursuant to his employment or contract with the Commission, or his employment with such contractor.

ACKNOWLEDGMENTS

The author is deeply indebted to Professor Howard K. Birnbaum for his advice, patience, guidance and active cooperation throughout the course of this investigation. He also wishes to record his appreciation to Professor C. J. Altstetter for his guidance and advice from time to time. He thanks Mr. Craig Baker for his active cooperation during the later part of the experiments.

TABLE OF CONTENTS

	Page
ACKNOWLEDGMENTS.	iii
I. INTRODUCTION.	1
II. EXPERIMENTAL PROCEDURE.	3
III. THEORY	7
IV. RESULTS AND DISCUSSION.	15
V. CONCLUSIONS	20
LIST OF REFERENCES	21

LIST OF FIGURES

		Page
1.	Block diagram of pulse-echo measuring circuit.	23
2.	Etch figure on (111) plane of Nb single crystal (x 400).	24
3.	Logarithmic decrement vs. frequency plotted in log-log scale. Both the specimens are zone-refined Nb single crystals containing about 10 ppm. N ₂ . The solid curve is the theoretical curve fitted to the data points.	25
4.	Plot of log Δ vs. log ω for Nb single crystal specimen 1A having 10 ppm. N ₂ . The solid curve is the theoretical plot	26
5.	Plot of log Δ vs. log ω for Nb single crystal specimen 1A containing 400 ppm. N ₂ . The solid curve is the theoretical plot.	27
6.	Plot of log Δ vs. log ω for Nb single crystal specimen 1B having 700 ppm. O ₂ . The solid curve is the theoretical plot.	28
7.	Plot of log Δ vs. log ω for Nb single crystal specimen 1B having 1000 ppm. O ₂ . The solid curve is the theoretical plot fitted to the data points.	29
8.	Plot of log Δ vs. log ω for the as-grown unirradiated and irradiated Nb single crystals	30
9.	Plot of shear modulus of elasticity vs. the interstitial concentration in the Nb specimens.	31

I. INTRODUCTION

The analogy between dislocation motion under an oscillatory stress and the forced vibration of a string in a viscous medium was originally proposed by Koehler¹ and extended by Granato and Lü²cke. Analysis of this model leads to two sources of damping: a frequency dependent damping caused by the interaction of the vibrating dislocation's strain field with phonons³ and a frequency independent "hysteretic" damping caused by the transient motion of the dislocations during breakaway from their pinning points. Both the frequency dependent damping and the hysteretic damping were shown to be amplitude dependent in the stress range where the breakaway of the dislocation from the pinning points takes place.^{4,5} The predictions of these calculations have been largely supported by measurements on f.c.c. metals. In particular, the frequency dependence of the damping was shown to agree with the calculations in the megacycle^{6,7,8} and kilocycle⁶ frequency ranges under conditions where the damping was amplitude independent.

The nature of the damping due to dislocations in b.c.c. metals has not been carefully investigated. It has been shown⁹ that dislocations contribute to the

damping and that they can cause amplitude dependent damping. However, the predictions of the vibrating string model of dislocation motion have not been tested in the case of b.c.c. metals. In view of the controversy about the magnitude of the Peierls stress in b.c.c. metals a comparison of damping data with the predictions of a theory based on a flexible dislocation line is particularly significant.

The purpose of the present work is to examine whether the frequency dependence of dislocation damping in a typical b.c.c. metal such as niobium agrees with that predicted by the theory based on the vibrating string model. The technique used was the pulse-echo technique in the frequency range 5 to 170 Mc/sec. The dislocation contribution to the damping was obtained by subtracting the damping due to sources other than dislocation from the total damping. Great care was taken to maintain a constant dislocation configuration during the experiment and to provide internal checks on the frequency dependence.

II. EXPERIMENTAL PROCEDURE

Specimen Preparation

Crystals were grown from Wah Chang Nb containing several hundred ppm. substitutional impurities in the form of a rod (1/2" dia.) by passing a heated zone whose temperature was about 2400°C along the solid rod. The vacuum was 10^{-8} torr. Several large grains formed, two of which were big enough to be used as specimens. These grains were cut out of the rod using spark cutting to minimize the damage and the ends were made flat and parallel to each other to within 5×10^{-5} inch by spark machining. The damaged layer was not removed, since the etching process decreased the flatness of the ends which was quite critical. Since we are looking at a bulk property, this rather high density of dislocations (in the damaged layer) in a relatively small fraction of the total volume should have an insignificant effect on the property. The specimen axis along which the sound wave was propagated was within 2° of a $\langle 110 \rangle$ direction.

A double crystal ultrasonic technique was employed whereby two quartz transducers were glued onto the flat ends of the specimen using Nonaq grease. One of them was used to transmit the stress pulse into the specimen

and the second to receive the pulses as they appeared on the other end. The schematic circuit used for the megacycle measurements is shown in Fig. 1. The echoes were displayed on the Hewlett-Packard 175 A scope and recorded with a 1782 A display scanner. A time mark generator was used to fix an accurate time axis for the recorded pattern of echoes. The amplitudes of the echoes were measured directly on the oscilloscope screen. Two sets of transducers were used: 3/8" dia, X-cut, 5 Mc/sec transducers; 3/8" dia, X-cut, 10 Mc/sec transducers. Each set was used at frequencies which were odd harmonics of the fundamental frequency to give a wide range of available frequencies. The accuracy of the technique was verified by repeating the damping measurement in the two identical specimens; by using different quartz transducers and by trying different types of bonds (Salol and Eastman 9-10). The amplitude independence of the damping was verified by changing the drive voltage.

After determining the frequency dependence of the damping in the as-grown crystals they were alloyed with oxygen and/or nitrogen by annealing in controlled atmospheres. The specimen temperature was measured with a disappearing filament type optical pyrometer, the corrections for nonblack body condition and absorption of the radiation by the window being applied. The equilibrium concentrations of nitrogen and oxygen in the Nb in

equilibrium with gaseous N_2 was calculated using data of Cost and Wert¹⁰ and Fromm and Jehn¹¹ and the alloy concentrations used are shown in Table 1.

TABLE 1
INTERSTITIAL SOLUTE CONCENTRATIONS

Specimen	Treatment	Atmosphere	Conc. O ppm. Atomic	Conc. N ppm. Atomic
1-A and 1-B	As grown 2400°C, 10^{-9} torr	Air	9.4	10.4
1-A	Annealed 1600°C, 10^{-9} torr	Air	16.8	440
1-B	Annealed 1520°C, 10^{-7} torr	Air	700	515
1-B	Annealed 1650°C, 10^{-6} torr	Air	1000	983
1-B	Annealed 1650°C, 8×10^{-6} torr	Air	8000	2779

The introduction of interstitial solutes served to increase the concentration of pinning points at the dislocations since the fraction of the solute sites at the dislocation which are occupied, C_i can be written:

$$C_i = C_o e^{B/kT}$$

where C_o is the solute concentration in the lattice and B is the binding energy of the interstitial solute to the

dislocation. At each concentration of interstitial solute the ultrasonic attenuation was measured as a function of frequency. The specimen containing 8000 ppm. of O_2 had much lower damping values than the other specimens and its damping was used to determine the damping due to sources other than dislocation motion. The background damping values thus established were subtracted from the total measured damping at each frequency to obtain the dislocation damping contribution. Attempts to establish the background damping by irradiation were not successful and will be described subsequently.

The dislocation densities were determined after the ultrasonic attenuation measurements were completed. The dislocation etch pitting technique was applied to the (111) using the procedure developed by Guberman.¹³ Sufficient depth of surface was removed to ensure that damage due to the cutting procedure was removed. Successive polishing to remove pits and re-etching produced identical patterns of triangular etch pits. An example of the etch pits observed is shown in Fig. 2. Etch pit counts were made from pictures of varying magnifications which were taken from the specimen after etching for different times. An average of the calculated dislocation densities was about $3-4 \times 10^4/cm^2$.

III. THEORY

The model analyzed by Koehler¹ and by Granato and Lücke² considers the dislocation lines in a crystal to be pinned at various points along their length by two kinds of pins. The first kind is a strong pin (such as a dislocation network intersection), from which the dislocation cannot break away; at least at stresses below the stress necessary for dislocation multiplication. The distance between these strong pins is called the network length. A real crystal will have a distribution of network lengths. Distributed along the dislocations is a second type of pin (breakable pin) with a much weaker, short range binding force to the dislocation. At sufficiently high stresses the dislocations can break away from these pins, and the resulting damping is then amplitude dependent. Vacancies or impurities would create pins of this type. The distance between breakable pins is called the loop length. A real crystal will also have a distribution of loop lengths as well as breakable pins with different binding energies to the dislocations. A dislocation moving in a crystal experiences a viscous drag due to phonon scattering and thermoelastic effects.

In the model suggested by Koehler¹ the dislocations are treated as extensible strings with a mass and line tension. It is also assumed that the dislocation line tension is independent of curvature and that the force opposing dislocation motion is a viscous drag proportional to the velocity.

For stresses below the stress required for break-away, the equation of motion for a loop of length l perpendicular to the applied stress is given by

$$A \frac{\partial^2 \xi}{\partial t^2} + B \frac{\partial \xi}{\partial t} - C \frac{\partial^2 \xi}{\partial x^2} = b \tau_0 \sin \omega t \quad (1)$$

with the boundary conditions

$$\xi(0, t) = \xi(l, t) = 0. \quad (2)$$

Here, ξ is the displacement normal to the x -axis, which lies along the dislocation line in the absence of an applied stress. The amplitude of the applied resolved shear stress is τ_0 and the angular frequency is ω . The mass of the dislocation per unit length A is taken approximately as $\rho \pi b^2$, where ρ is the density and b is the Burger's vector. The viscous damping force is $B \frac{\partial \xi}{\partial t}$. The effective dislocation line tension is $C = \frac{2Gb^2}{(1-\nu)\pi}$, where G is the shear modulus and ν is Poisson's ratio. The solution to (1) can be found by assuming a solution of the form

$$\xi(x, t) = \sum_{n=0}^{\infty} \sin \frac{n\pi x}{l} (R_n \cos \omega t + S_n \sin \omega t) \quad (3)$$

and solving for the constants R_n and S_n . The solution found in this way is

$$\xi(x,t) = \frac{4b\tau_0}{A} \sum_{n=0}^{\infty} \left[(w_{2n+1}^2 - w^2) + \frac{B^2 w^2}{A^2} \right]^{-\frac{1}{2}} \cdot \frac{1}{2n+1} \cdot \sin \frac{(2n+1)\pi x}{l} \sin(\omega t + \gamma_{2n+1}), \quad (4)$$

$$\text{where, } w_{2n+1} = \left(\frac{C}{A}\right)^{\frac{1}{2}} \frac{(2n+1)\pi}{l}$$

and

$$\gamma_{2n+1} = \tan^{-1} \left(\frac{\frac{B}{A} w}{w^2 - w_{2n+1}^2} \right)$$

The logarithmic decrement is defined as $\frac{W}{2W}$, where W is energy dissipated per unit volume per cycle. The vibrational energy W is given by $W = \frac{\tau_0^2}{2M}$, where M is the appropriate elastic modulus. Since we are considering a shear stress on the dislocation, the appropriate modulus is the shear modulus G . The energy loss per cycle for one loop of length l is equal to

$$4 \int_0^l dx \int_0^{\frac{\pi}{2w}} B \cdot \frac{\partial \xi}{\partial t} \cdot \frac{\partial \xi}{\partial t} \cdot dt \quad (5)$$

For N dislocation loops of length l per unit volume,

$$\Delta(l) = \frac{\delta W}{2W} = \left(\frac{8Gb^2}{\pi A} \right) (Nl) \sum_{n=0}^{\infty} \frac{1}{(2n+1)^2}$$

$$\left[\frac{\frac{B}{A} w}{(w_{2n+1}^2 - w^2)^2 + \left(\frac{B}{A} w \right)^2} \right] \quad (6)$$

The quantity w_1 is of order 2×10^8 cps but because B/A is of order 2×10^{10} , the resonance is overdamped, and the maximum in $\Delta(l)$ occurs at $w \sim 10^7$ cps. Thus for frequencies less than 2×10^8 cps, the series for $\Delta(l)$ converge very rapidly and only the first term need be used. This may then be more conveniently written in the form

$$\Delta(l) = 8Nl \frac{Gb^2}{\pi^3 C} l^2 \left[\frac{\omega \tau}{1 + \omega^2 \tau^2} \right] \quad (7)$$

where w = frequency of the applied stress

and τ = relaxation time = $\frac{Bl^2}{\pi^2 C}$

The longitudinal crystal strain due to dislocation motion will cause an apparent change in Young's modulus, which for N dislocation loops of length l per unit volume is given by

$$\frac{\delta E}{E}(l) = \left(\frac{8Gb^2}{\pi A} \right) (Nl) \sum_{n=0}^{\infty} \frac{1}{(2n+1)^2}$$

$$\left[\frac{w_{2n+1}^2 - w^2}{(w_{2n+1}^2 - w^2)^2 + \left(\frac{Bw}{A} \right)^2} \right] \quad (8)$$

For frequencies less than 2×10^8 c.p.s., the series for $\frac{\delta E}{E} (l)$ converges very rapidly and only the first term need be used.

$$\frac{\delta E (l)}{E} = \frac{8 N(l) b^2 G l^2}{\pi^4 C} \left[\frac{1}{1 + \omega^2 \tau^2} \right] \quad (9)$$

In a real crystal where a loop length distribution $N(l)$ exists,

$$\Delta = \int_{l_{\min}}^{l_{\max}} \Delta (l) N (l) dl \quad (10)$$

and

$$\frac{\delta E}{E} = \int_{l_{\min}}^{l_{\max}} \frac{\delta E (l)}{E} N (l) dl$$

where l_{\min} . and l_{\max} . are minimum and maximum loop lengths in the distribution. The damping resulting from a random distribution of breakable pins has been calculated by Trott⁴ for all concentrations of breakable pins. For large number of randomly placed breakable pins per network length he showed that the loop length distribution obtained approaches the exponential distribution originally proposed by Koehler:

$$N (l) dl = \frac{\Delta}{L^2} e^{-\frac{l}{L}} dl \quad (11)$$

where Ω is the total length of movable dislocation per unit volume, and L is the average loop length ($L = \frac{\Delta}{N}$). Using this loop length distribution in (6) for Δ (1), the result for frequencies well below the maximum is

$$\Delta = \frac{960 \Omega G b^2 \Lambda L^4 B \omega}{\pi^5 c^2}$$

$$\frac{\delta E}{E} = \frac{48 \Omega G b^2 \Lambda L^2}{\pi^4 c} \quad (12)$$

Thus when the measuring frequency is on the low frequency side of the maximum, (7) predicts that the damping should be directly proportional to frequency and extrapolate to zero for $\omega = 0$. Similar considerations (12) predicts that modulus defect $\frac{\delta E}{E}$ should be frequency independent at frequencies below the maximum.

The dislocations in a crystal are distributed over all the possible slip systems, and therefore the results must be integrated over all the possible dislocation orientations with respect to the applied stress in the crystal system being considered.

$$\Delta = \sum_k \Omega_k \Delta_k \quad (13)$$

Ω_k & Δ_k are respectively the orientation factor and decrement corresponding to the k^{th} slip system. The

right hand side of (10) must therefore be multiplied by an orientation factor Ω .

At

$$w_{\max} = \frac{0.084 \pi^2 C}{L^2 B} \quad (14)$$

the damping reaches a maximum value

$$\Delta_{\max} = \frac{17.6 \Omega G b^2 \Lambda L^2}{\pi^3 C} \quad (15)$$

for an exponential loop length distribution. The values for a delta function loop length distribution are

$$\begin{aligned} w_{\max} &= \frac{1}{\tau} = \frac{\pi^2 C}{B L^2} \\ \& \quad \Delta_{\max} &= 4 \Omega \frac{G b^2}{\pi^3 C} \Lambda L^2 \end{aligned} \quad (16)$$

The damping at $w \gg w_{\max}$ is given by

$$\Delta = \frac{8 \Lambda G b^2}{\pi B w} \quad (18)$$

for all loop length distributions. The damping should thus be proportional to $1/w$ at frequencies above the maximum.

If Δ_{\max} is multiplied by w_{\max} ,

for an exponential loop length distribution.

Therefore:

$$B = \frac{14.59 \Omega G b^2 \Delta}{\Delta_{\max} \omega_{\max}} \quad (20)$$

From a knowledge of the parameters on the right hand side, the damping constant (B) can be calculated.

In the present experiment the attenuation of a sound wave $\alpha(\omega)$ is measured. This is related to the decrement (Δ) by:

$$\alpha = \frac{\Delta \omega}{0.722} = 8.68 f \Delta \quad (21)$$

where f is the frequency expressed in megacycles per second.

IV. RESULTS AND DISCUSSION

The as-grown Nb single crystal specimens containing 10 ppm. N_2 exhibited a w^{-1} dependence of dislocation damping on frequency as shown in Fig. 3. The magnitude of the damping was about the same in both specimens. The results indicate that $w_{\max} < 5$ Mc/sec for these specimens. Increasing the concentration of breakable pins by alloying with oxygen and nitrogen gave the results shown in Figs. 4 to 7. As the solute concentration was increased, a maximum in the dislocation damping was observed at ~ 15 Mc/sec. On the high frequency side of the maximum, the data are linearly dependent on w^{-1} and within the experimental scatter agree with the values obtained for as-grown specimens containing 10 ppm. N_2 . On the high frequency side of the maxima therefore $\Delta \propto \omega^{-1}$; and is independent of loop length as predicted by the string model. The curves shown in Figs. 4 to 7 are calculated from the string model, (7), using an exponential loop length distribution. The values of w_{\max} and Δ_{\max} for each solute concentration are given in Table II.

TABLE 2

DAMPING PARAMETERS

Specimen No.	Solute Conc	Δ_{\max}	w_{\max} (Mc/sec)	B (c.g.s. units)
1A	400 ppm.N ₂	1.2×10^{-2}	1.05	8.36×10^{-5}
1B	700 ppm.O ₂	7×10^{-3}	3.5	8.86×10^{-5}
1B	1000 ppm.O ₂	3.7×10^{-3}	7	1.81×10^{-4}

It may be noted that the value of Δ_{\max} decreases as the loop length is decreased (by increasing the nitrogen concentration) and that the value of w_{\max} shifts toward higher frequencies as the loop length decreases. There is not sufficient data on the low frequency side of the maximum to test the validity of the model in this frequency range. Measurements in the kilocycle frequency range are needed for that purpose.

The damping constant B can be calculated from the following relationship:

$$B = \frac{14.59 \Omega G b^2 \Lambda}{\Delta_{\max} w_{\max}} \quad (22)$$

Taking $G = 2.87 \times 10^{11}$ dynes/cm², $b = 2.859 \times 10^{-8}$ c.m. and $\Omega = 1/10$ (factor of 2 uncertainty)

$\Lambda = 4 \times 10^4$ /cm² as indicated by the etch pit counts:

$$B = \frac{2.175 \times 10^{-6}}{f_m \Delta_m} \quad (23)$$

where, Δ_m is the maximum dislocation damping

and f_m is the frequency in Mc/sec.

The values of 'B' calculated from the data are shown in Table 2. It is seen that B is about 9×10^{-5} c.g.s. units.

Leibfreid's³ formula for damping constant is

$$B = \frac{3kTZ}{10 C_T a^2}$$

where, T = temp in absolute scale

k = Boltzmann's constant

Z = number of atoms per unit lattic cell

C_T = shear velocity corresponding to

$$\left[\frac{C_{44} (C_{11} - C_{12})}{2} \right]^{\frac{1}{2}}$$

a = lattic parameter

Taking T = 300°k, Z = 2

$$C_T = 2.16 \times 10^5 \text{ cm./sec.},^{12} \quad a = 3.3 \times 10^{-8} \text{ cm.}$$

B is calculated to be $\sim 10^{-4}$ c.g.s. units, which agrees with the experimental value.

The Granato-Lücke model (9) predicts a $\frac{1}{\omega^2}$ dependence of $\frac{\delta E}{E}$ on the high frequency side of the damping maxima i.e., for $\omega\tau \gg 1$. The experimental data shown in Fig. 8 suggests that $\frac{\delta E}{E}$ is independent of frequency within experimental error ($\sim 2\%$) for a given concentration of interstitials in the specimen. This indicates that the contribution to modulus defect due to dislocation motion is small. The vibrating string model results in $\frac{\delta E}{E} \sim \Delta$ and since Δ is less than 10^{-2} the modulus defects due to dislocation motion is within the experimental error. As shown in Fig. 9 the modulus did increase as the interstitial solute concentration increased. The modulus defect in a specimen having a certain concentration of interstitials is found to be frequency independent.

One of the as-grown Nb single crystals (1A) was given progressively higher neutron doses up to 1.26×10^{16} neutrons/cm² (1.5 MeV). But no significant effect on the dislocation damping of material was observed as shown in Fig. 9. This suggests either of two possibilities:

- (1) The neutron dose given cannot produce sufficient number of point defects to pin the dislocations, or
- (2) The point defects produced do not migrate to the dislocations. In a recent paper, Guberman¹³ reports an increase in lattice resistance to dislocation mobility

caused by neutron irradiation of Nb single crystals. The neutron doses that Guberman employed are comparable with that employed in the present work. This indicates that a neutron dose of the order of 10^{16} neutrons/cm² (> 1.5 MeV) produces interstitials which are sufficient in number to impede the motion of dislocations. Therefore, it may be inferred that while sufficient point defects to pin the dislocations are produced in the lattice by the neutron dose employed, a large fraction of them do not imigrate to dislocations.

V. CONCLUSIONS

It has been shown that the vibrating string model of dislocation damping can account for the magnitude of the internal friction in Nb in the megacycle frequency range. The data for the frequency dependence of logarithmic decrement fit the theoretical curve for the exponential loop length distribution deduced from the Granato-Lücke model. The damping constant was calculated from measurements of the frequency and damping of the maximum of the damping vs. frequency curve and from dislocation etch pit measurements. The experimental value of B was 9×10^{-5} c.g.s. units. The value of 'B' thus obtained agrees with that deduced from Leibfreid's formula. It was observed that neutron irradiation did not change the values of damping in the megacycle frequency range for doses less than 1.26×10^{16} neutrons/cm². The damping was influenced by the addition of interstitial solutes in a manner which is consistent with interstitial solute pinning of the dislocations.

LIST OF REFERENCES

1. J. S. Koehler, Imperfections in nearly perfect crystals (John Wiley & Sons, Inc., New York, 1953), p. 197.
2. A. Granato & K. Lü^ucke, J. Appl. Phys. 27, 583(1956).
3. G. Leibfried, Z. Physik. 127, 344 (1950).
4. B. D. Trott, Ph.D. thesis (University of Illinois, 1966).
5. D. H. Rogers, J. Appl. Phys. 33, 781 (1962).
6. C. R. Heiple & H. K. Birnbaum, J. Appl. Phys, 38, 3294 (1967).
7. R. M. Stern & A. V. Granato, Acta Met, 10, 358 (1962).
8. G. A. Alers & D. O. Thomson, J. Appl. Phys, 32, 283 (1961).
9. R. H. Chambers, Physical Acoustics, Vol. III, part A, 123.
10. J. Cost & C. A. Wert, Acta Met., 11, 231 (1963).
11. E. Fromm & H. Jehn, Zeitschrift Für Metallkunde, 58, 61 (1967).
12. D. I. Bolef, J. Appl. Phys., 32, 100 (1961).
13. H. D. Guberman, Acta Met, 16, 713 (1968).

FIGURE CAPTIONS

- Fig. 1 Block diagram of pulse-echo measuring circuit.
- Fig. 2 Etch figure on (111) plane of Nb single crystal (x 400).
- Fig. 3 Logarithmic decrement vs. frequency plotted in log-log scale. Both the specimens are zone-refined Nb single crystals containing about 10 ppm. N_2 . The solid curve is the theoretical curve fitted to the data points.
- Fig. 4 Plot of $\log \Delta$ vs. $\log \omega$ for Nb single crystal specimen 1A having 10 ppm. N_2 . The solid curve is the theoretical plot.
- Fig. 5 Plot of $\log \Delta$ vs. $\log \omega$ for Nb single crystal specimen 1A containing 400 ppm. N_2 . The solid curve is the theoretical plot.
- Fig. 6 Plot of $\log \Delta$ vs. $\log \omega$ for Nb single crystal specimen 1B having 700 ppm. O_2 . The solid curve is the theoretical plot.
- Fig. 7 Plot of $\log \Delta$ vs. $\log \omega$ for Nb single crystal specimen 1B having 1000 ppm. O_2 . The solid curve is the theoretical plot fitted to the data points.
- Fig. 8 Plot of $\log \Delta$ vs. $\log \omega$ for the as-grown unirradiated and irradiated Nb single crystals.
- Fig. 9 Plot of shear modulus of elasticity vs. the interstitial concentration in the Nb specimens.

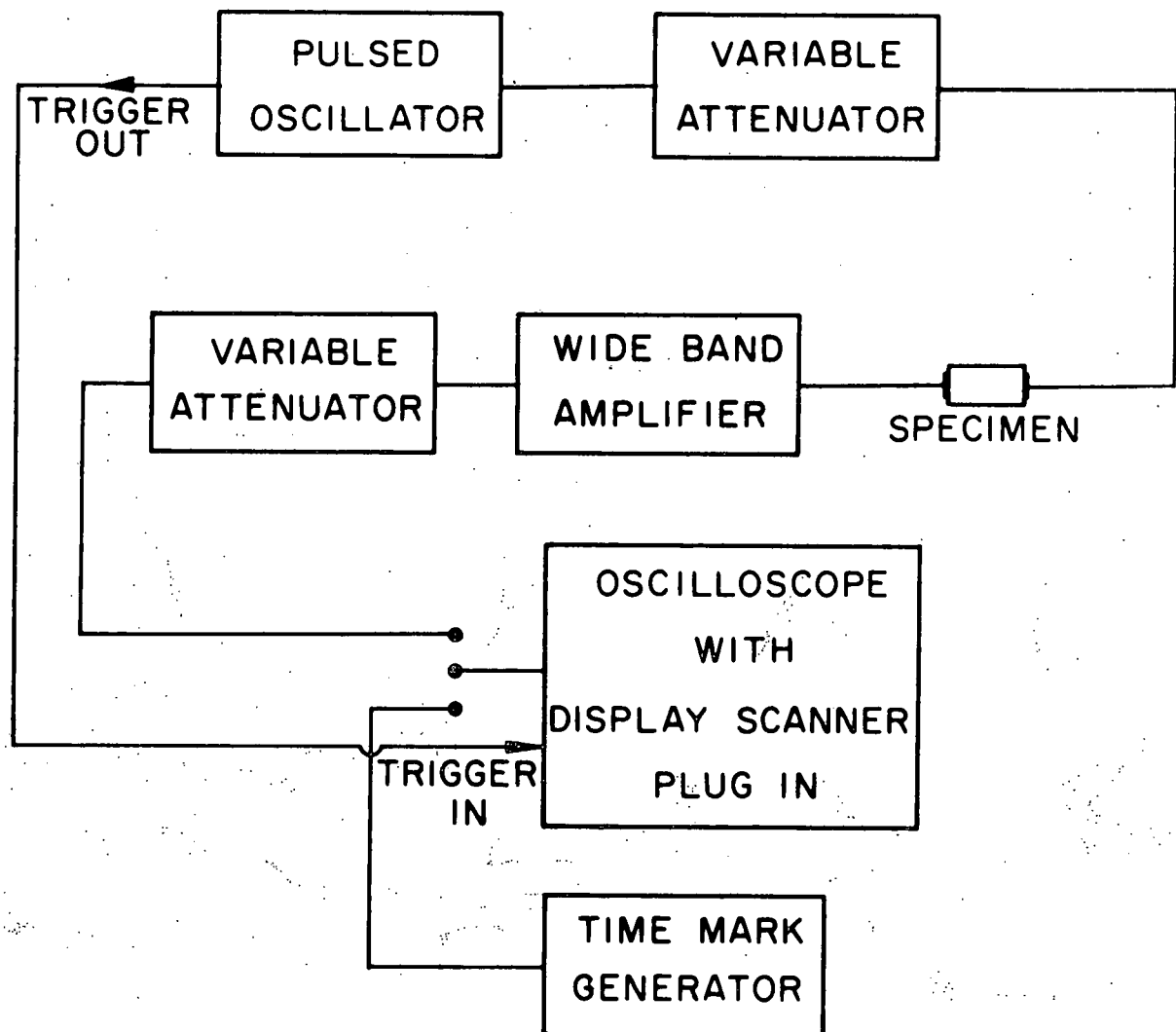


FIG. 1

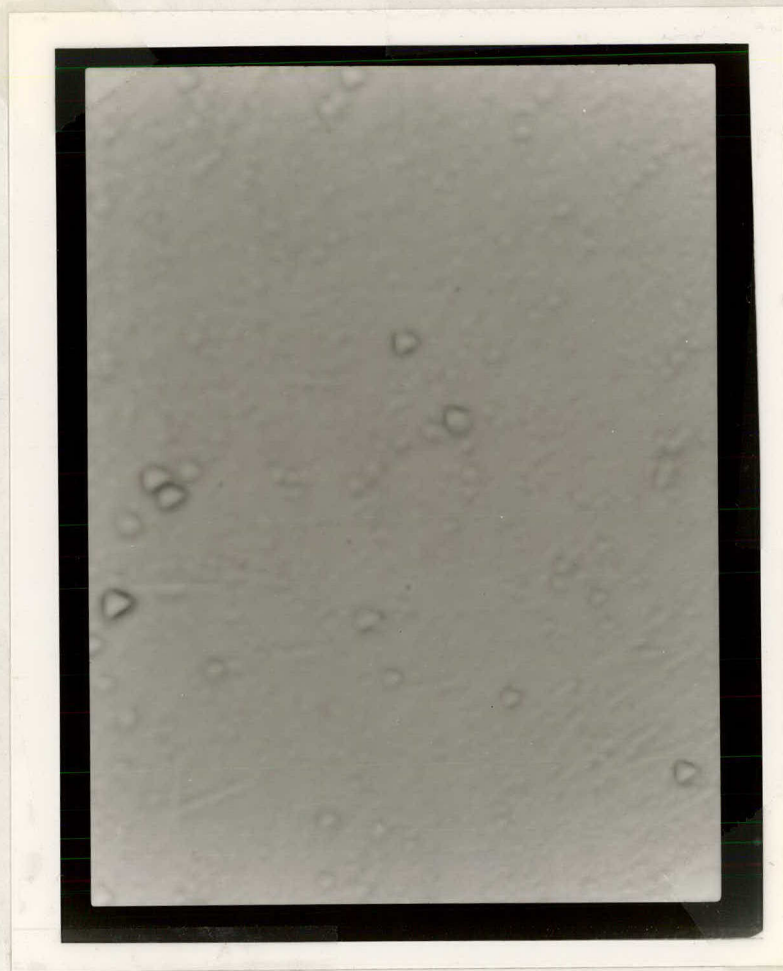


FIG. 2

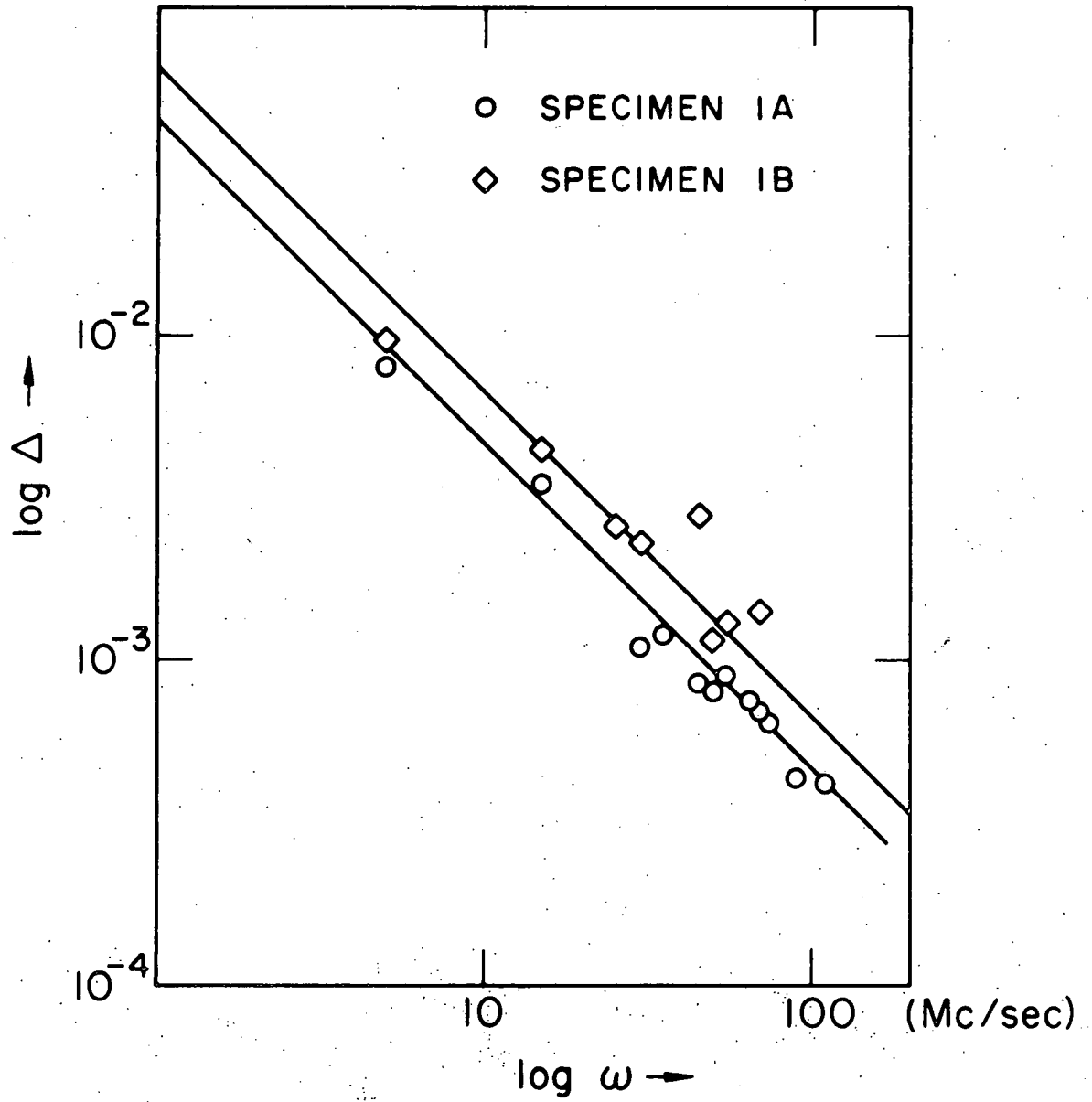


FIG. 3

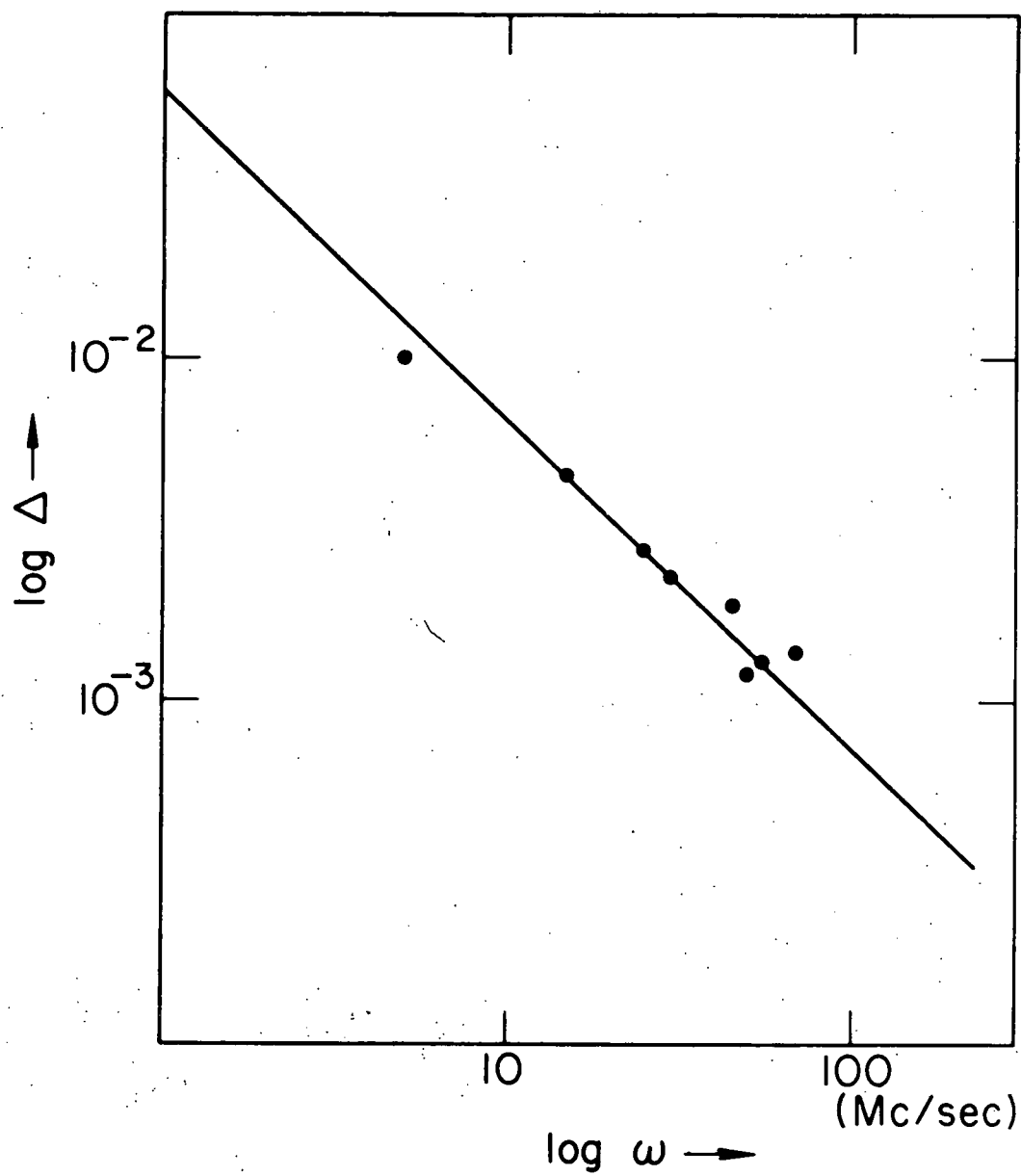


FIG. 4

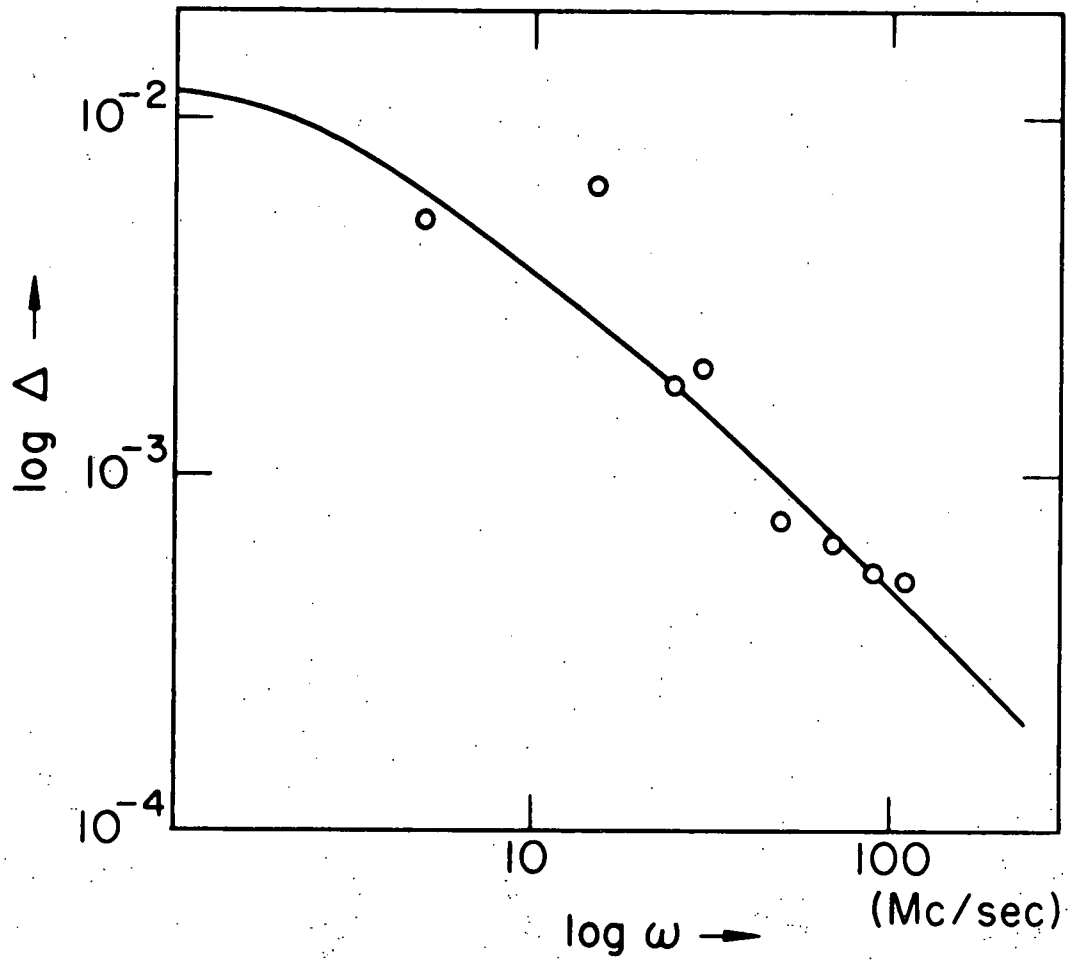


FIG. 5

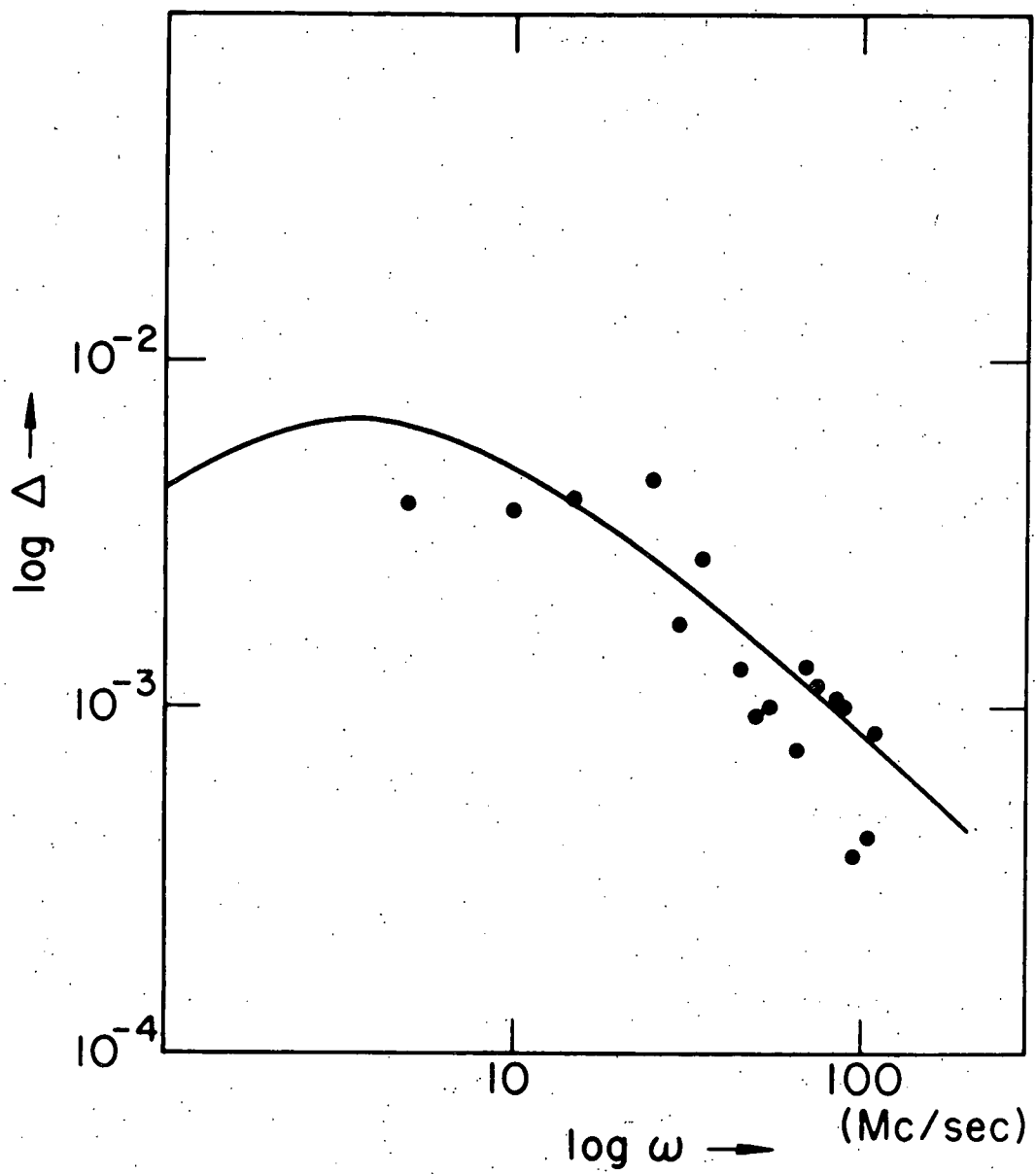


FIG. 6

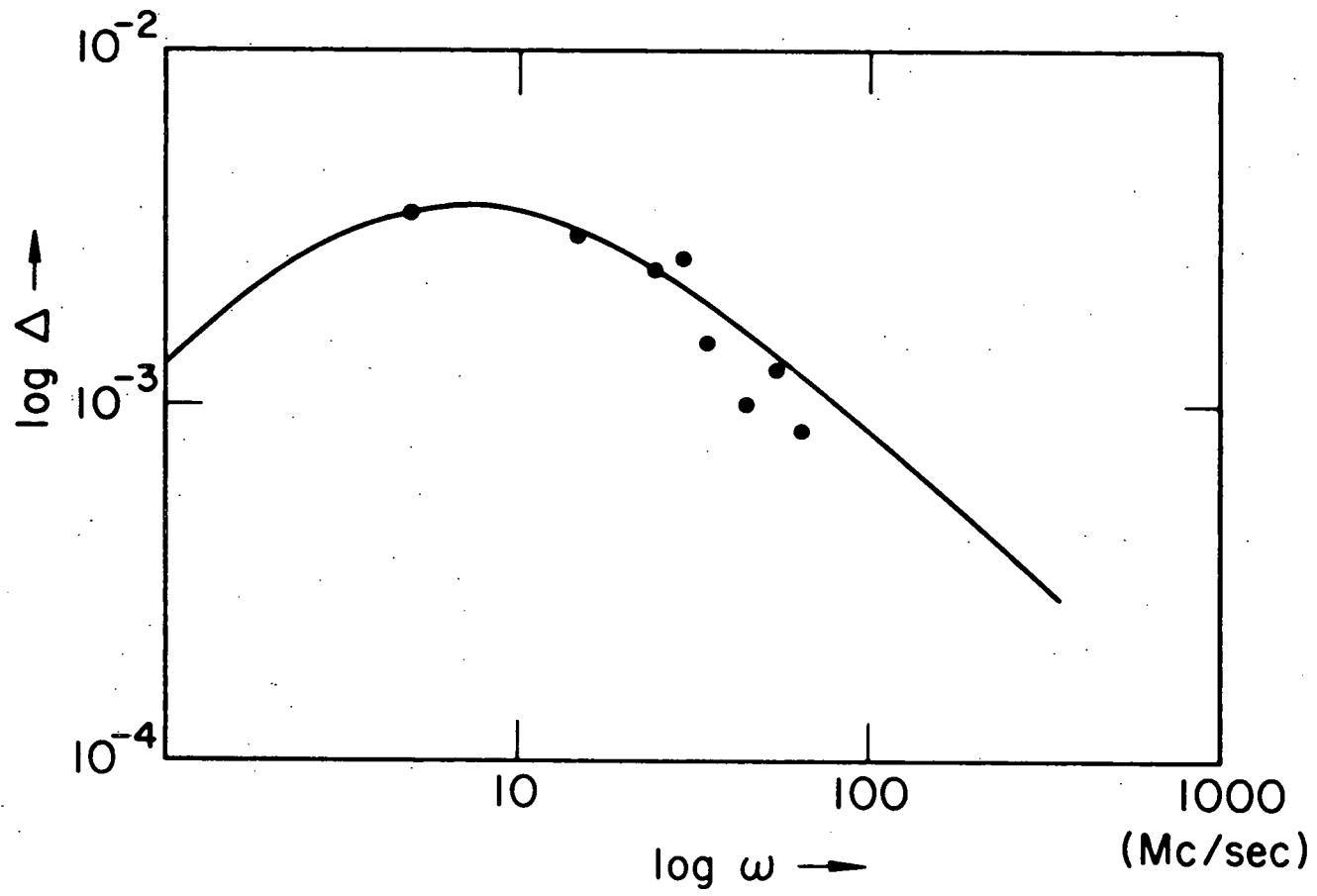


FIG. 7

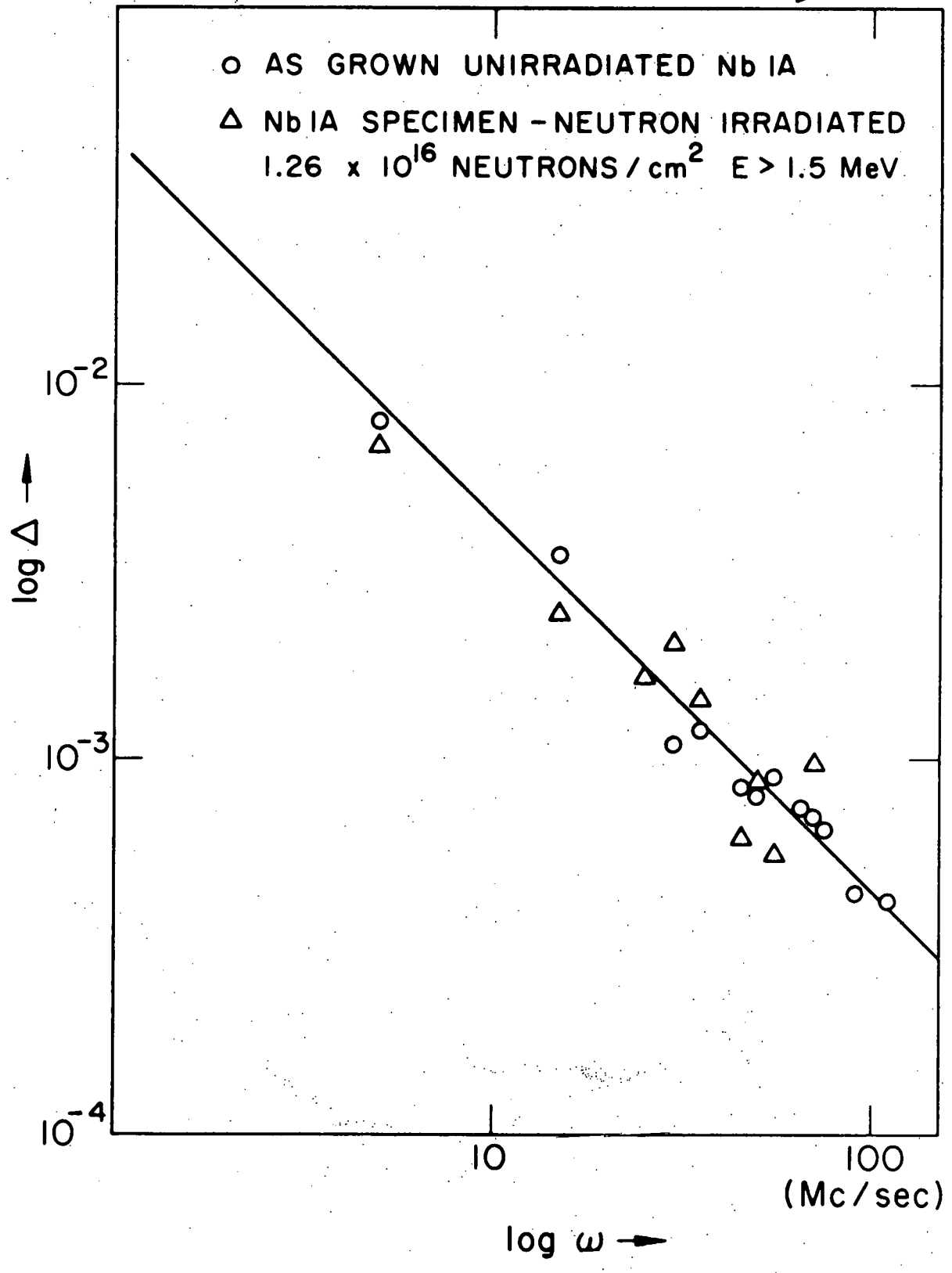


FIG. 8

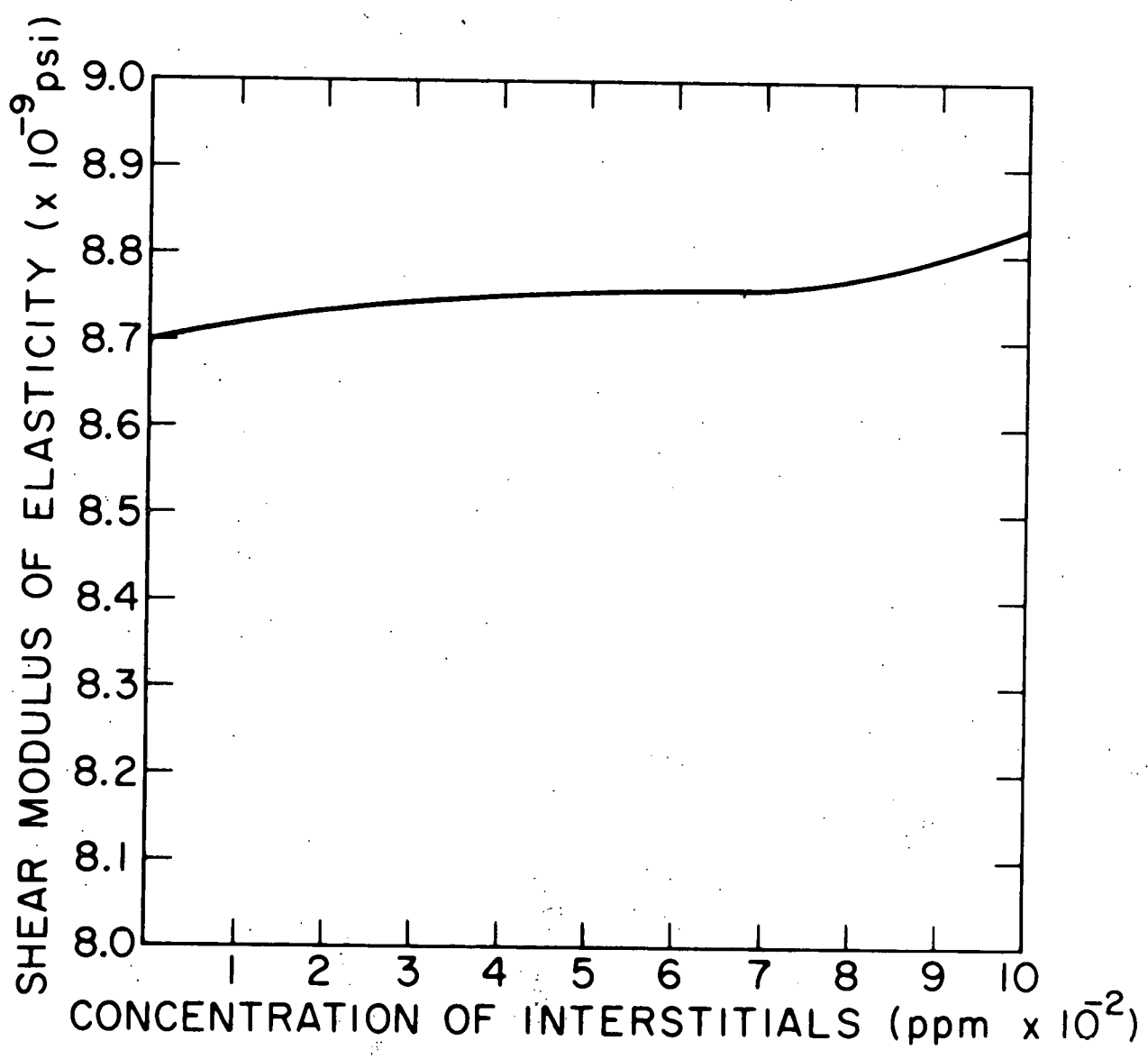


FIG. 9